Cuckoo search algorithm and particle swarm optimization based maximum power point tracking techniques

Sally Abdulaziz, Galal Attlam, Gomaa Zaki, Essam Nabil
Department of Industrial Electronics and Control Engineering, Faculty of Electronic Engineering, Menoufia University, Menoufia, Egypt

Article Info	ABSTRACT
	Increasing the efficiency of photovoltaic (PV) systems is a pressing issue, and several studies have focused on the maximum power point tracking (MPPT) techniques to extract the maximum PV output power. Many MPPT techniques have been discussed in the last decade, and optimization-based MPPT techniques have shown better performance than other MPPT techniques. In this study, two optimization techniques, the cuckoo search algorithm and particle swarm optimization with changing inertia weight techniques, are discussed and applied to a PV system to track the maximum power point. The MSX-60 PV module and boost DC-DC converter are used in this paper to simulate and model the MPPT system using MATLAB/Simulink to show which technique has the best performance under various solar irradiation scenarios. In addition, different structures of PV arrays such as series-parallel, bridge link, and total cross-tied PV structures are simulated to analyze their effect on the efficiency of MPPT processes.

Corresponding Author:

Sally Abdulaziz
Department of Industrial Electronics and Control Engineering
Faculty of Electronic Engineering, Menoufia University
Menoufia, Egypt
Email: sally.abdulaziz@yahoo.com

1. INTRODUCTION

The burning of fossil fuels has many disastrous effects on our environment as it causes greenhouse gas emission, which causes global climate change and the formalization of atmospheric aerosols, increasing the global mortality rate [1]. Burning 1 L of fossil fuels can emit approximately 2.9 KG of greenhouse gases [2]. Besides, if the use of nonfossil fuel resources is increased by 1%, the emission of carbon dioxide decreases by 0.8% [3]. In addition to environmental pollution, fossil fuels are limited, whereas energy demands increase as the world population grows; it is predicted to increase by 65% in 2030 [4].

Based on these, there is an urgent need to use renewable energy sources, such as hydropower, geothermal, solar, biomass, and solar resources. Renewable energy has many advantages: it is free, clean, green, and environmentally friendly as it does not cause any greenhouse gas emissions or air pollution [5]. Besides the environmental benefits of renewable energies, there are economic benefits, as the use of renewable energy can reduce the dependence on imported fossil fuels. In contrast to conventional energy resources, renewable energy resources do not deplete. Thus, renewable energy is the best energy resource to tackle the environmental and economic challenges faced due to the generation of electricity.

One of the most favorable resources of renewable energy is solar energy. It can be used directly to heat water for households, reducing power consumption by 13% [6]. Electricity can be generated from solar

energy using either a direct or an indirect method. The direct method uses photovoltaic (PV) systems, and the indirect method uses optical devices that provide steam to propel a turbine and generate electricity [7]. PV systems are preferred as they generate no noise, have low preservation expenditure, and can be installed in urban areas close to the loads [8], so they are considered as distributed generation (DG) [9]. The most crucial advantage of DG is power saving because, during the transmission of power from the power source to the consumers, up to 13% of the generated energy can be lost due to the joule effect [10].

Despite the advantages of PV systems, the conversion efficiency of PV arrays is extremely low [11] and dependent on atmospheric conditions [12], and they have high installation costs [13]. To reduce their cost of generating 1 kWh, the PV systems effectiveness must be increased using a dynamic tracking algorithm to track the maximum power point (MPP), especially when solar radiation and ambient temperature change. There are two types of MPP trackers (MPPTs): mechanical and electronic trackers. Mechanical trackers direct the PV panel to track the sun using single or dual-axis trackers [14]. Electronic trackers are preferred due to the disadvantages of such tracers, including complexity, low efficiency, and high cost. There are many MPPT algorithms that can be categorized into three classes: conventional, soft computing, and optimization-based MPPTs. These algorithms differ in convergence speeds, complexity, accuracy, steady-state and dynamic efficiencies, number of sensors used in the algorithm, and costs [15]. Many studies have compared the listed techniques [16]–[21], and others have improved the existing MPPT algorithms to improve their efficiency [22]–[26]. Optimization-based MPPT algorithms have been reported to have a better performance than the conventional techniques, especially under partial shading conditions (PSC) [27]–[29], as the conventional techniques are a local MPP (LMPP) and cannot track the global MPP (GMPP).

Many researchers implement particle swarm optimization (PSO) and Cuckoo search algorithm (CSA) algorithms to track the MPP, as shown in [30], [31]. It is noted that the PSO algorithm is not very efficient in tracking the MPP, so a PSO algorithm with a changing inertia weight strategy is used to enhance the algorithm's efficiency and is discussed in this paper. In this paper, PSO with changing inertia weight and CSA algorithms are compared to show which one is more efficient in tracking MPP. In addition, different structures of PV arrays and their effect on the efficiency of MPPT processes are compared. The rest of this paper is arranged as follows: Section 2 describes a PV system; Section 3 presents MPPT techniques; Section 4 presents the simulation results; Section 5 presents the concluding remarks. The references are listed in the final section.

2. PV SYSTEM
2.1. PV array modeling
PV cells are the essential components of a PV array. The most popular single-diode PV cell (Figure 1) is composed of a diode in parallel with a photocurrent source in addition to series and shunt resistances. These resistances can be neglected for simplicity.
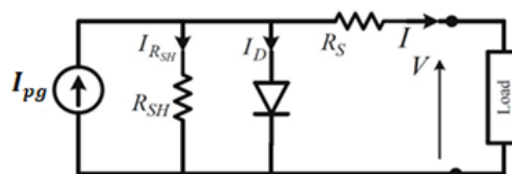

Figure 1. PV cell model

The output current of a PV array can be expressed as [32]:

$$i_{opv} = N_{pc}I_{pg} - N_{sc}I_{rsc}\left[\exp\left(\frac{k_{pv}v_{opv}}{N_{sc}}\right) - 1\right] \tag{1}$$

where i_{opv} is the PV-array output current, N_{sc} and N_{pc} the number of series and parallel PV cells, respectively, $\boldsymbol{I_{pg}}$ the photogenerated current, and I_{rsc} the reverse saturation current.

$$k_{pv} = {q_c}/{(I_f K_B T_a)} \tag{2}$$

Where q_c is the electron charge ($q_c = 1.6 \times 10^{-19}$ C), K_B the Boltzmann's constant ($K_B = 1.3805 \times 10^{-23}$ J/K), T_a the ambient temperature, and I_f the ideality factor of the p–n junction. The reverse saturation current is calculated using the (3):

$$I_{rsc} = I_{rrs} \left(\frac{T_a}{T_{ra}}\right)^3 exp\left[q_c E_{gb}(1/T_{ra}) - (1/T_a)/I_f K_B\right] \tag{3}$$

where T_{ra} is the reference temperature, I_{rrs} the reverse saturation current at T_{ra}, E_{gb} the bandgap energy ($E_{gb} = 1.1 \ eV$). The photogenerated current is calculated as (4):

$$I_{pg} = \left(I_{scc} + K_{It}(T_a - T_{ra})\right)\frac{s_r}{100} \tag{4}$$

where I_{scc} is the short-circuit current, K_{It} the short-circuit current temperature coefficient, s_r the solar irradiance. The output power is calculated using (5).

$$P_{opv} = i_{opv} v_{opv} = N_{pc} I_{pg} v_{opv} - N_{pc} I_{rsc} v_{opv} \left(\exp\left(\frac{k_{pv} v_{opv}}{N_{sc}}\right) - 1\right) \tag{5}$$

As MPP occurs at $dp_{opv}/dv_{opv} = 0$, the following Equation can be used to calculate the maximum output voltage.

$$exp\left(\frac{k_{pv} v_m}{N_{sc}}\right)\left[\left(\frac{k_{pv} v_m}{N_{sc}}\right) + 1\right] = \frac{I_{pg} + I_{rsc}}{I_{rsc}} \tag{6}$$

Where v_m is the maximum output voltage. Solving these equations with variation in solar irradiance (s_r), the PV-array characteristics can be plotted as shown in Figure 2. Figure 2(a) represents the P-V characteristics, and the I-V characteristics are shown in Figure 2(b).
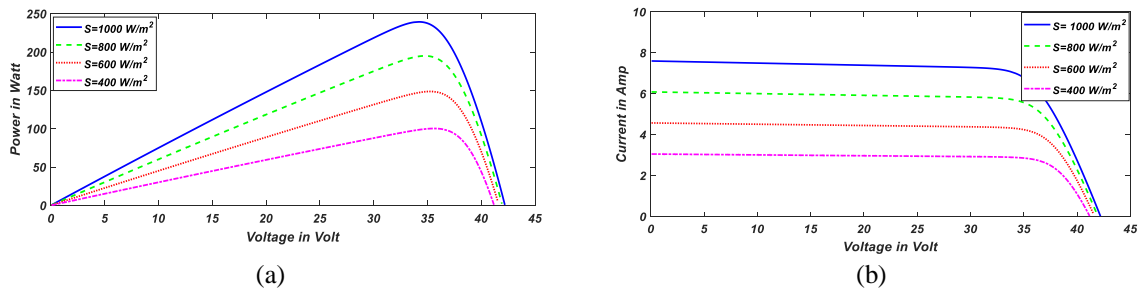

Figure 2. PV characteristics under uniform solar irradiance levels: (a) P–V and (b) I–V characteristics

Figure 2 shows the PV characteristics under uniform solar irradiance, but the PV array may be operated under PSC due to buildings, clouds, or dust in natural conditions. Thus, the PV-array characteristics change, and several peaks are obtained, as shown in Figure 3. Figure 3(a) represents the P-V characteristics, and the I-V characteristics are shown in Figure 3(b).
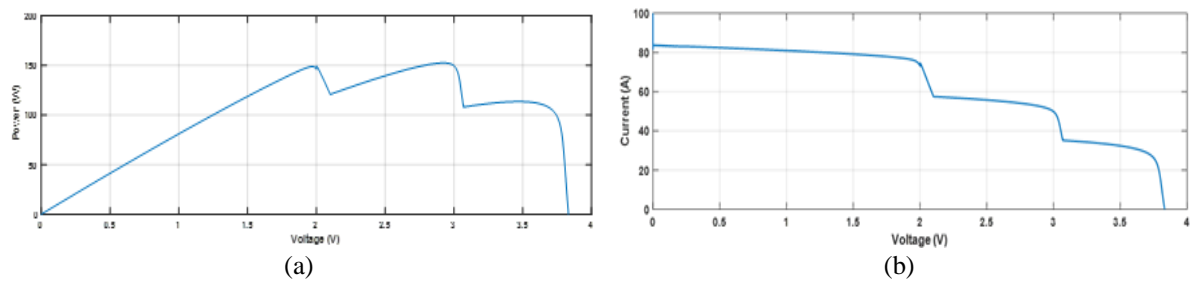

Figure 3. PV characteristics under PSC: (a) P–V and (b) I–V characteristics

Because the amount of power generated by a PV cell is small, cells can be connected in parallel or series to produce a higher current or voltage, respectively. A PV module is obtained by connecting several PV cells. Many modules can be connected to construct a PV array to produce the desired voltage and current. PV arrays are connected using three methods [33] (Figure 4). Figure 4(a) represents the series-parallel (SP) structure, Figure 4(b) represents the bridge-link (BL) structure, and the total cross-tied (TCT) structure is shown in Figure 4(c).
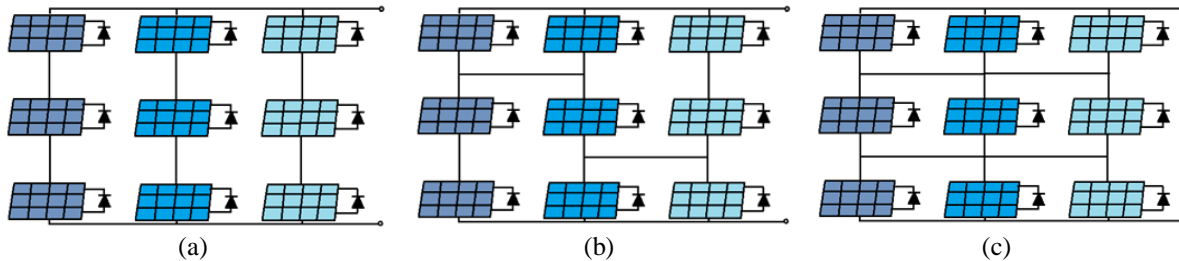
| (a) | (b) | (c) |

Figure 4. PV-array structures: (a) SP, (b) BL, and (c) TCT structures

Modules in the SP structure are connected in series, and each series string is connected in parallel with other strings. Each module in the TCT structure is linked in series and parallel with other modules. The BL structure is intermediate between the SP and TCT structures. PSC impacts the short circuit current of the modules, which affects the output current of the modules at their MPP, resulting in a poor cohesiveness between the MPPs of the modules and the MPP of the array. Because the TCT structure has far more parallel interlinkages than the SP structure, more current paths are provided to avoid the current decrease due to the current decrease in other branches [34]. The TCT structure's parallel interconnections may also decrease the probability of turning on bypass diodes, thereby avoiding their relating losses [35].

2.2. DC-DC boost converter

The output voltage of the boost converter is always higher than the input voltage, so it may be called a step-up converter. Figure 5 shows a DC-DC boost converter topology. The boost converter consists of a voltage source, an inductor, a capacitor, a diode, a switch, and load resistance.
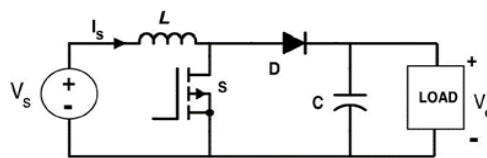
Figure 5. Boost converter topolog

The switch (S) can be closed or opened to obtain the desired output voltage. The relationship between the input and output voltages is expressed as (7):

$$V_o = \frac{V_s}{1-D} \tag{7}$$

where V_s is the converter's input voltage, V_o is the converter's output voltage, D is the converter's duty cycle.

The (8) can be used to calculate the average inductor current.

$$I_L = \frac{V_s}{(1-D)^2 R} \tag{8}$$

Because the output voltage and inductor current depend on the duty cycle, the operational status of the boost converter can be controlled by adjusting the duty cycle. An MPPT technique is used to control this duty cycle, obtain the desired voltage, and get the boost converter to operate the PV system at the voltage at which MPP occurs.

3. MPPT TECHNIQUES

The maximum power of a PV system can be extracted using MPPT techniques irrespective of the atmospheric conditions. MPPT uses an electronic system to change the electrical operating point of a PV module to deliver maximum power. The schematic diagram of a PV system with the MPPT technique is presented in Figure 6. In this section, CSA and PSO algorithms are discussed as they have been proven to be more efficient than other techniques
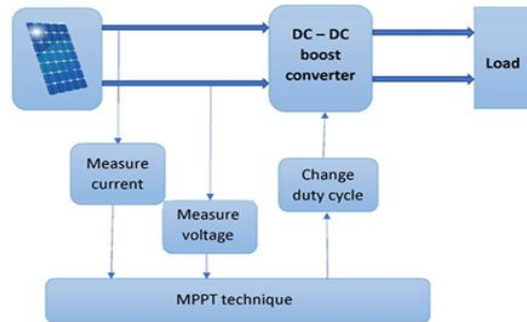

Figure 6. Schematic diagram of MPPT

3.1. Cuckoo search algorithm (CSA)

Yang and Deb developed CSA in 2009 [36]. It is a metaheuristic algorithm inspired by the breeding strategy of cuckoo birds. The CSA algorithm is explained in detail in the flow chart in Figure 7 and the few lines below. Cuckoo birds lay their own eggs on other birds' (host birds) nests. To enhance the reproduction possibility of their own eggs, cuckoo birds may throw away one of the host birds' eggs to lay their own egg instead of the thrown egg. Cuckoo eggs are often very similar to those of the host birds, except they are slightly bigger. Cuckoo eggs are hatched before the host birds' eggs, and once the cuckoo chicks are hatched, they expel the host bird's eggs from the nest to increase their feeding chance. The host bird can discover the cuckoo eggs with the possibility p_a, where $p_a \in [0,1]$. When the host bird discovers cuckoo eggs, it either destroys them or relinquishes the nest to build another one.

Looking for the host nests is similar to the process of searching for food. It is found that Drosophila melanogaster and fruit flies search the landscape using a sequence of straightforward flight directions interrupted by a rapid 90° shift, which leads to the lévy flight style [37]. In CSA, the eggs in the nest are referred to as solutions, and the cuckoo egg is the new solution. The new nests are generated by the lévy flight are expressed as (9):

$$x_i^{(t+1)} = x_i^{(t)} + \alpha \oplus l\,\acute{e}vy(\lambda), \tag{9}$$

where $x_i^{(t+1)}$ is the new solution, $x_i^{(t)}$ the current solution, α the step size ($\alpha > 0$), and $\oplus$ the entry wise multiplication. $l\,\acute{e}vy(\lambda)$ can be determined as (10):

$$l\,\acute{e}vy(\lambda) \approx u = l^{-\lambda}, \tag{10}$$

where $1 < \lambda < 3$.

The (11) represents a simple scheme of the lévy distribution:

$$s \approx K \left(\frac{u}{(|v|)^{1/\beta}}\right)(x_{best} - x_i) \tag{11}$$

u, v denote the normal distribution curves where:

$$u = N(0, \sigma_u^2), v = N(0, \sigma_v^2) \tag{12}$$

where σ_u, σ_v can be defined by (13):

$$\sigma_u = \left[\frac{\gamma(1+\beta) \times sin(\pi \times \beta/2)}{\gamma\left(\frac{1+\beta}{2}\right) \times \beta \times 2^{\frac{\beta-1}{2}}}\right]^{1/\beta}, \sigma_v = 1 \tag{13}$$

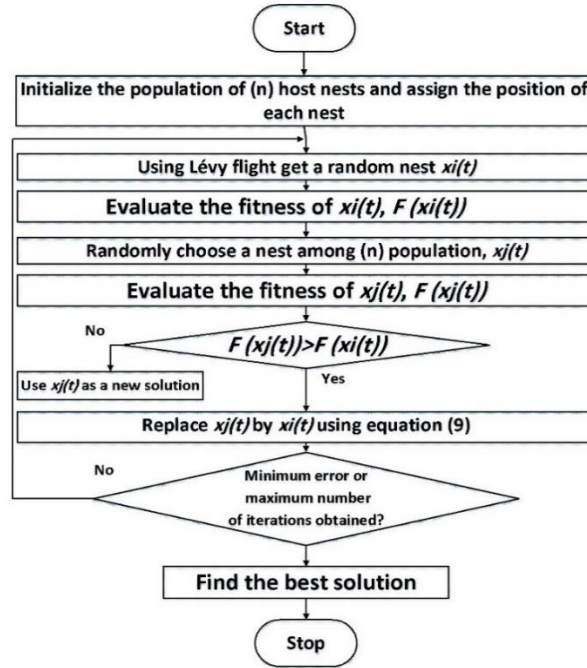where γ is the integral gamma function.

Figure 7. Flowchart of the CSA algorithm

In MPPT, the converter's duty cycle is represented by the nest position, whereas the fitness evaluation function represents the PV-generated power which is represented in (5).

3.2. Particle swarm optimization (PSO)

PSO is a swarm-based algorithm introduced by Kennedy and Eberhart [38]. PSO is employed in many applications because it is accurate, reliable, easy to implement, requires only a small calculational memory [39]. PSO algorithm is explained in detail in the flow chart shown in Figure 8 and the following few lines. PSO was inspired by a biological herd of birds seeking food in a specific area. In PSO, the herd is called the "swarm", and the birds are called "particles." First, the swarm is initialized in the search space with several particles in random positions. These particles search for the optimum solution. Each particle's position and velocity are updated after each iteration based on (14) and (15):

$$s_i(t+1) = \omega(t+1) * s_i(t) + C_1 r_1 (p_{best} - l_i(t)) + C_2 r_2 (g_{best} - l_i(t)), \qquad (14)$$

$$l_i(t+1) = l_i(t) + s_i(t+1), \qquad (15)$$

where $s_i(t+1)$ is the current velocity; $s_i(t)$ the previous velocity; $l_i(t+1)$ is the current position; $l_i(t)$ is the previous position of particle i; $r_1 \ and \ r_2$ are random numbers ($r_1, r_2 \ \epsilon \ [0,1]$); $C_1 \ and \ C_2$ are the cognitive learning rates; $\omega(t+1)$ is the inertia weight in the current iteration; p_{best} is the best position achieved by the particle; g_{best} is the best position achieved by the particles' neighbors. ω can be obtained using (16):

$$\omega_{iter} = \omega_{max} - \frac{\omega_{max} - \omega_{min}}{iter_{max}} * iter, \qquad (16)$$

where ω_{max} is the maximum inertia weight ($\omega_{max} = 0.9$), ω_{min} the minimum inertia weight ($\omega_{min} = 0.4$), $iter$ the number of the current iteration, and $iter_{max}$ the maximum number of iterations. From (13), it is evident that the inertia weight is at its maximum value at the beginning of the iterations to accelerate the velocity of the particles, which can enhance the global search ability and reach the optimal solution fastly. During the iterations, the value of inertia weight is reduced gradually, which results in enhancing the local search ability and reaching the optimal solution. After updating each particle's position and velocity, the fitness evaluation function is calculated. If the fitness value of the updated particle is better than the memorized personal best position (p_{best}), p_{best} is adjusted to make it equal to the position of the current particle, and the same steps are iterated for the global best position (g_{best}). In MPPT, the particle position represents the converter's duty cycle, whereas, the fitness evaluation function represents the PV-generated power which is represented in (5).
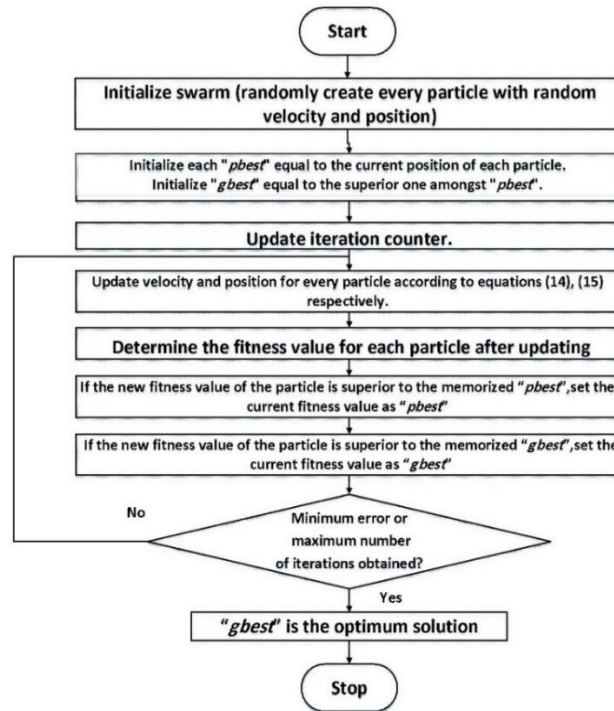
Figure 8. Flowchart of the PSO algorithm

3.3. Parameter values

The parameters of metaheuristic algorithms have a significant effect on their performance. As a result, the choice of these parameters must be done carefully. The parameter values for both algorithms are shown in Table 1.

Table 1. The parameter values used for both algorithms

CSA		PSO	
Population size	6	Population size	6
Number of iterations	200	Number of iterations	200
p_a	0.25	ω_{min}	0.4
α	1	ω_{max}	0.9
β	1.5	$c_1 = c_2$	0.8
K	0.1	$r_1 = r_2$	1

4. SIMULATION RESULTS

The MATLAB/Simulink program was used to build a 3×3 MSX-60 PV array to analyze the effectiveness of the MPPT techniques for different PV structures. Four cases were simulated, as shown in Figure 9. Case 1 is represented in Figure 9(a), case 2 is represented in Figure 9(b), case 3 is represented in Figure 9(c), and case 4 is represented in Figure 9(d). For every case, PSO and CSA were tested, and the output PV power for every case is shown in Table 2.

Case 1: the standard conditions (STC). In this case, the PV array has been tested with different PV structures under STC. The results for this case are represented in Figure 10, Figure 10(a), Figure 10(b), and Figure 10(c) represent SP, BL, and TCT structures, respectively.

Case 2: PSC with bottom shading. In this case, the PV array has been tested under PSC with different irradiation levels. The three upper PV modules were irradiated with 1000 W/m^2, the three middle modules were irradiated with 900 W/m^2 and the three bottom modules were irradiated with 700 W/m^2. Results for this case are represented in Figure 11, Figure 11(a), Figure 11(b), and Figure 11(c) represent SP, BL, and TCT structures, respectively.

Case 3: PSC with side shading. In this case, the PV array has been tested under PSC with different irradiation levels. The three top PV modules were irradiated with 900 W/m^2, the three middle modules were irradiated with 700 W/m^2 and the three bottom modules were irradiated with 500 W/m^2. The results for this case are represented in Figure 12, Figure 12(a), Figure 12(b), and Figure 12(c) represent SP, BL, and TCT structures, respectively.

Case 4: In this case, the upper left side of the array was irradiated with 700 W/m^2, and the rest of the array was irradiated with 500 W/m^2. The results for this case are represented in Figure 13, Figure 13(a), Figure 13(b), and Figure 13(c) represent SP, BL, and TCT structures, respectively.
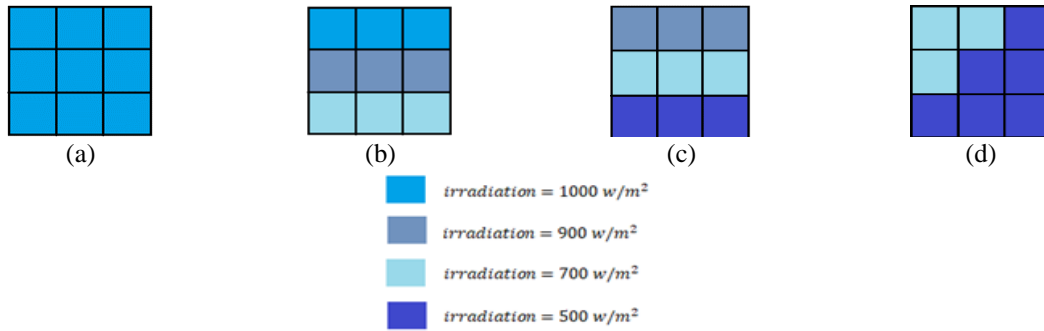

Figure 9. Different solar irradiation scenarios: (a) standard condition (STC), (b) PSC with higher irradiance, (c) PSC with lower irradiance, and (d) uniform low solar irradiance
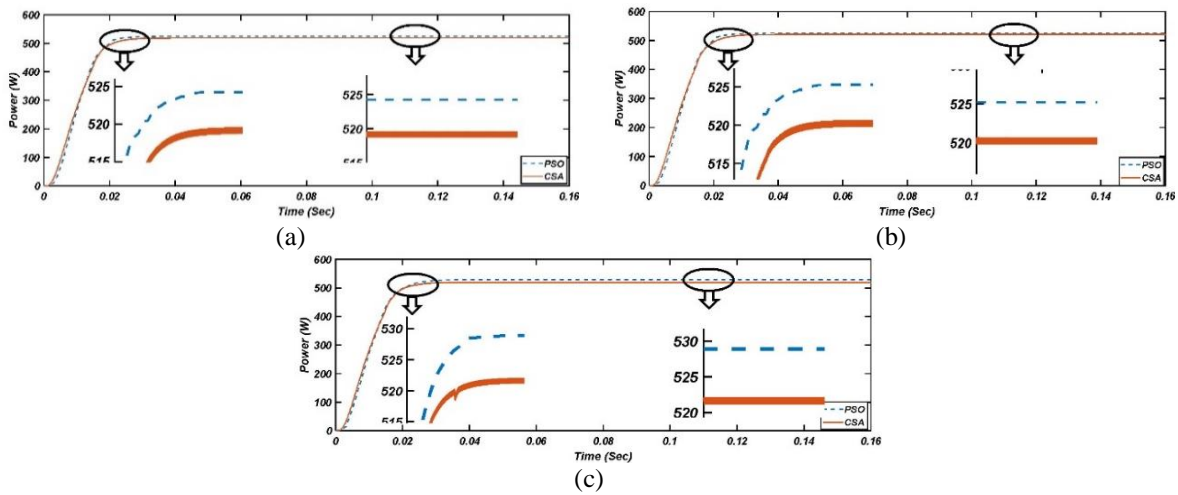

Figure 10. Comparison between PSO and CSA performance for Case 1 for different PV structures: (a) SP, (b) BL, and (c) TCT
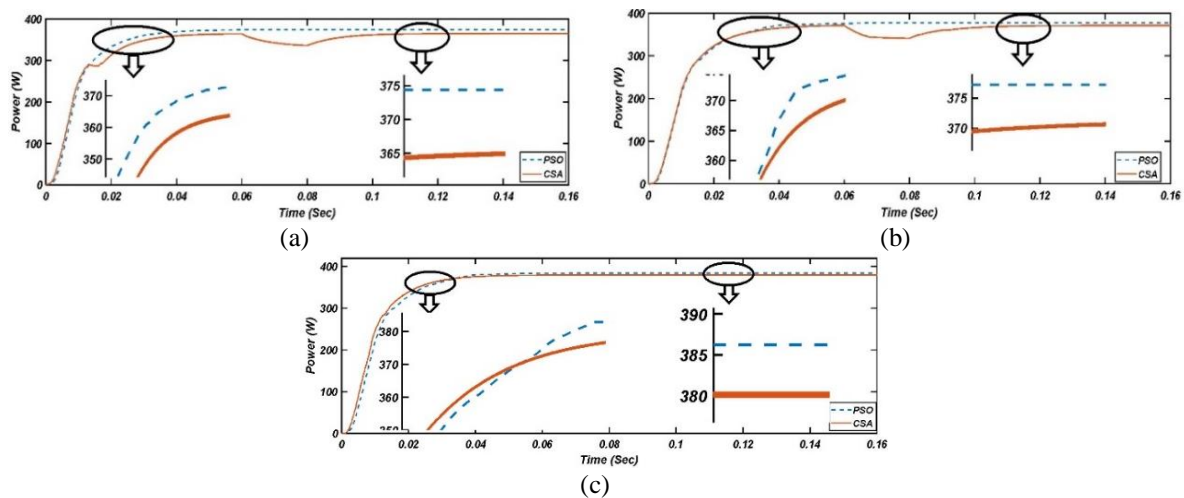

Figure 11. Comparison between PSO and CSA performance for case 2 for different PV structures: (a) SP, (b) BL, and (c) TCT
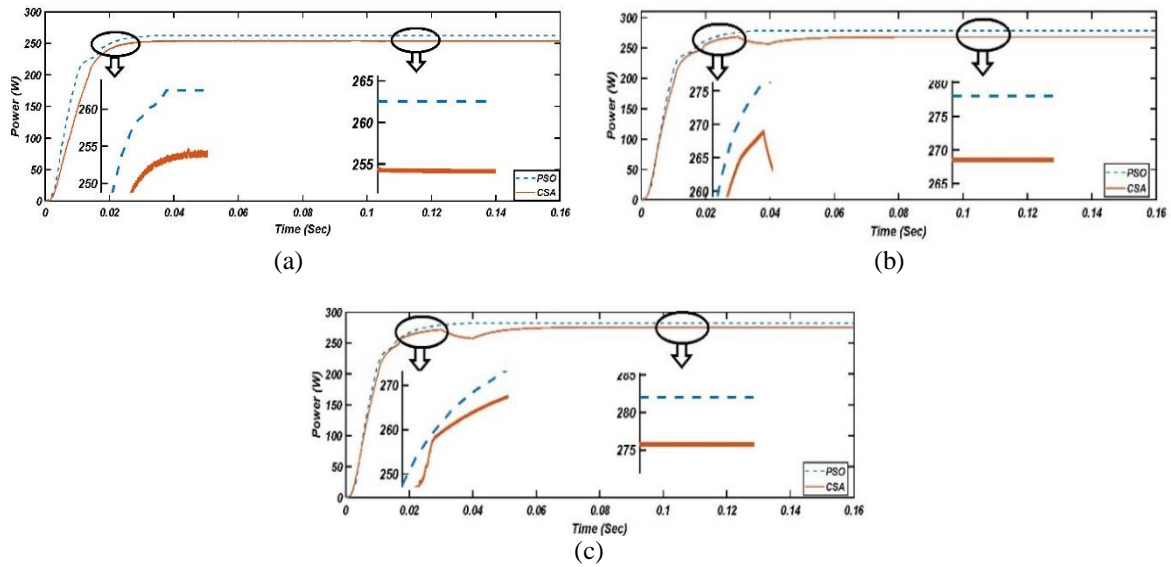
(a)

(b)

(c)

Figure 12. Comparison between PSO and CSA performance for case 3 for different PV structures: (a) SP, (b) BL, and (c) TCT
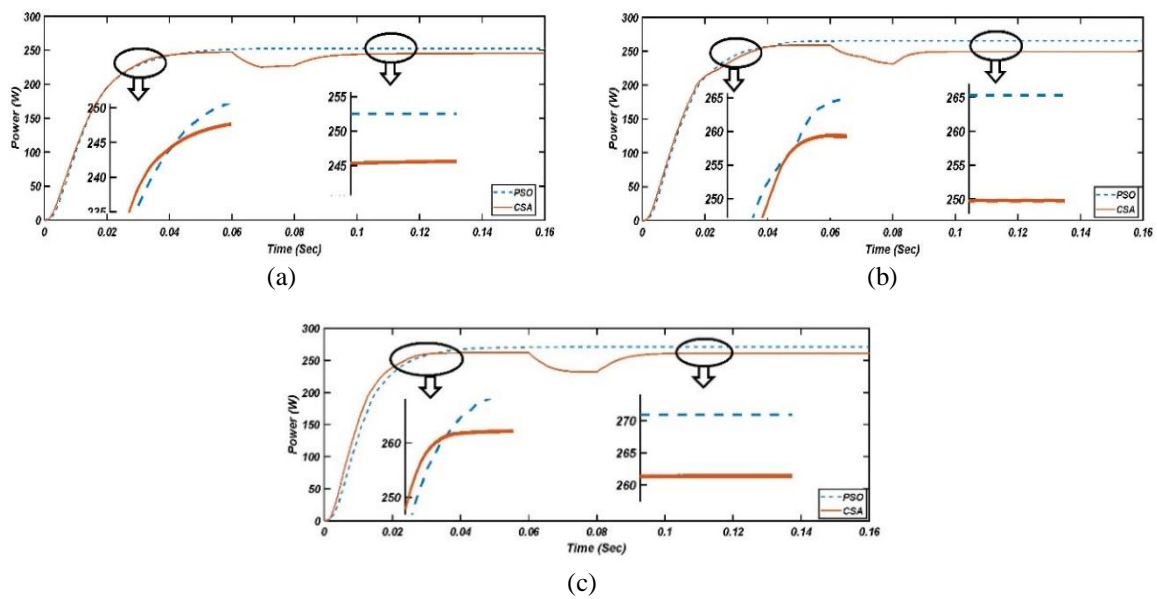

(a)

(b)

(c)

Figure 13. Comparison between PSO and CSA performance for case 4 for different PV structures: (a) SP, (b) BL, and (c) TCT

PSO algorithm has many advantages, such as being accurate, reliable, stable, easy to implement, few parameters to be determined, and efficient in global search; also CSA algorithm has many advantages, such as requiring only a few parameters to be tuned, and the performance of the CSA algorithm doesn't depend heavily on the value of the parameter p_a. However, both parameters have serious drawbacks, such as their relatively slow convergence speed; also CSA algorithm can easily fall into local optimal solution.

The simulation results show that the PSO algorithm is more efficient and stable than the CSA technique in all tested cases. Obviously, the PSO algorithm has a faster response in most tested cases than the CSA algorithm. The simulation results also indicated that the efficiency of the TCT PV structure appears especially under SPC. The stability of both algorithms is tested across different runs, each algorithm is executed for each tested case, and the variance of solutions is computed using MATLAB's var function, and the results are shown in Table 3. From the variance results, it is obvious that both algorithms have good stability across different runs, but PSO is more stable than CSA in most of the tested cases.

Table 2. The PV output power (W) for each case

Cases	Technique	SP	BL	TCT
Case 1	CSA	519.21	521.50	521.91
	PSO	524.16	525.54	528.13
Case 2	CSA	365.30	371.47	380.21
	PSO	374.58	376.93	386.13
Case 3	CSA	254.87	269.9	275.3
	PSO	262.45	278.16	282.69
Case 4	CSA	245.67	249.96	261.54
	PSO	252.53	265.28	270.96

Table 3. The variance of output power across different runs for each case

Cases	Technique	SP	BL	TCT
Case 1	CSA	0.0037	0.00023	0.002
	PSO	0.00038	0.00013	0.0018
Case 2	CSA	4.4532	0.05	0.0430
	PSO	0.00033	0.00055	0.00042
Case 3	CSA	0.0063	0.00025	0.0063
	PSO	0.00018	1.6849	0.00067
Case 4	CSA	0.0025	0.0039	8.008
	PSO	0.00015	0.00037	0.00053

5.   CONCLUSION

In this study, two optimization-based MPPT techniques were developed, CSA and PSO, and simulated them in a PV system using the MATLAB/Simulink program to determine the effectiveness of each technique under various atmospheric conditions. The simulation results showed that the PSO technique is more efficient and stable than the CSA technique under all tested conditions. The simulation results also indicated that varying the PV-array structure can affect the efficiency of the PV system, and the TCT structure is more efficient than other PV structures, especially under PSC. However, as explained in the following sentences, adapting both algorithms into the PV system presents numerous challenges. Although the PSO algorithm tracks the MPPT faster than the CSA algorithm, the PSO algorithm's convergence speed is still relatively slow. Although both algorithms achieve excellent stability across different runs in most tested cases, they can fall into the local optimal solution, and the result is not assured to be the global optimal solution. Finally, both algorithms heavily depend on their parameter values, and changing the parameter values will definitely change the result.

REFERENCES

[1]   D. Shindell and C. J. Smith, "Climate and air-quality benefits of a realistic phase-out of fossil fuels," *Nature*, vol. 573, no. 7774, pp. 408–411, Sep. 2019, doi: 10.1038/s41586-019-1554-z.
[2]   Ü. Ağbulut and S. Sarıdemir, "A general view to converting fossil fuels to cleaner energy source by adding nanoparticles," *International Journal of Ambient Energy*, vol. 42, no. 13, pp. 1569–1574, Jan. 2021, doi: 10.1080/01430750.2018.1563822.
[3]   B. Liddle and P. Sadorsky, "How much does increasing non-fossil fuels in electricity generation reduce carbon dioxide emissions?," *Applied Energy*, vol. 197, pp. 212–221, Jul. 2017, doi: 10.1016/j.apenergy.2017.04.025.
[4]   A. Qazi *et al.*, "Towards sustainable energy: a systematic review of renewable energy sources, technologies, and public opinions," *IEEE Access*, vol. 7, pp. 63837–63851, 2019, doi: 10.1109/ACCESS.2019.2906402.
[5]   Y. Liang, B. Yu, and L. Wang, "Costs and benefits of renewable energy development in China's power industry," *Renewable Energy*, vol. 131, pp. 700–712, Feb. 2019, doi: 10.1016/j.renene.2018.07.079.
[6]   E. Aydin, P. Eichholtz, and E. Yönder, "The economics of residential solar water heaters in emerging economies: The case of Turkey," *Energy Economics*, vol. 75, pp. 285–299, Sep. 2018, doi: 10.1016/j.eneco.2018.08.001.
[7]   E. F. Camacho, M. Berenguel, I. Alvarado, and D. Limon, "Control of solar power systems: a survey," *IFAC Proceedings Volumes*, vol. 43, no. 5, pp. 817–822, 2010, doi: 10.3182/20100705-3-be-2011.00135.
[8]   P. G. V. Sampaio and M. O. A. González, "Photovoltaic solar energy: conceptual framework," *Renewable and Sustainable Energy Reviews*, vol. 74, pp. 590–601, Jul. 2017, doi: 10.1016/j.rser.2017.02.081.
[9]   K. Tanaka *et al.*, "Decentralised control of voltage in distribution systems by distributed generators," *IET Generation, Transmission and Distribution*, vol. 4, no. 11, pp. 1251–1260, 2010, doi: 10.1049/iet-gtd.2010.0003.
[10] U. Sultana, A. B. Khairuddin, M. M. Aman, A. S. Mokhtar, and N. Zareen, "A review of optimum DG placement based on minimization of power losses and voltage stability enhancement of distribution system," *Renewable and Sustainable Energy Reviews*, vol. 63, pp. 363–378, Sep. 2016, doi: 10.1016/j.rser.2016.05.056.
[11] K. W. Nasser, S. J. Yaqoob, and Z. A. Hassoun, "Improved dynamic performance of photovoltaic panel using fuzzy logic-MPPT algorithm," *Indonesian Journal of Electrical Engineering and Computer Science*, vol. 21, no. 2, pp. 617–624, Feb. 2020, doi: 10.11591/ijeecs.v21.i2.pp617-624.
[12] S. K. Gopalakrishnan, S. Kinattingal, and S. P. Simon, "MPPT in PV systems using PSO appended with centripetal instinct attribute," *Electric Power Components and Systems*, vol. 48, no. 9–10, pp. 881–891, Jun. 2020, doi: 10.1080/15325008.2020.1825552.
[13] J. Ahmed and Z. Salam, "An improved perturb and observe (P&O) maximum power point tracking (MPPT) algorithm for higher efficiency," *Applied Energy*, vol. 150, pp. 97–108, Jul. 2015, doi: 10.1016/j.apenergy.2015.04.006.
[14] C. Alexandru, "Multi-body system simulation of the sun trackers used for PV panels," *IOP Conference Series: Materials Science and Engineering*, vol. 568, no. 1, Aug. 2019, p. 12001, doi: 10.1088/1757-899X/568/1/012001.
[15] M. Abdel-Salam, M. T. EL-Mohandes, and M. Goda, "History of maximum power point tracking," in *Green Energy and Technology*, Springer International Publishing, 2020, pp. 1–29.
[16] C. H. Basha and C. Rani, "Different conventional and soft computing MPPT techniques for solar PV systems with high step-up boost converters: A comprehensive analysis," *Energies*, vol. 13, no. 2, p. 371, Jan. 2020, doi: 10.3390/en13020371.
[17] R. B. Bollipo, S. Mikkili, and P. K. Bonthagorla, "Critical review on PV MPPT techniques: Classical, intelligent and optimisation," *IET Renewable Power Generation*, vol. 14, no. 9, pp. 1433–1452, Jun. 2020, doi: 10.1049/iet-rpg.2019.1163.
[18] S. Motahhir, A. El Hammoumi, and A. El Ghzizal, "The most used MPPT algorithms: review and the suitable low-cost embedded board for each algorithm," *Journal of Cleaner Production*, vol. 246, p. 118983, Feb. 2020, doi: 10.1016/j.jclepro.2019.118983.

[19]   A. Ali *et al.*, "Investigation of MPPT techniques under uniform and non-uniform solar irradiation condition-a retrospection," *IEEE Access*, vol. 8, pp. 127368–127392, 2020, doi: 10.1109/ACCESS.2020.3007710.

[20]   S. H. Hanzaei, S. A. Gorji, and M. Ektesabi, "A scheme-based review of MPPT techniques with respect to input variables including solar irradiance and PV arrays' temperature," *IEEE Access*, vol. 8, pp. 182229–182239, 2020, doi: 10.1109/ACCESS.2020.3028580.

[21]   J. S. Ko, J. H. Huh, and J. C. Kim, "Overview of maximum power point tracking methods for PV system in micro grid," *Electronics (Switzerland)*, vol. 9, no. 5, p. 816, May 2020, doi: 10.3390/electronics9050816.

[22]   S. Padmanaban, N. Priyadarshi, M. S. Bhaskar, J. B. Holm-Nielsen, V. K. Ramachandaramurthy, and E. Hossain, "A hybrid ANFIS-ABC based MPPT controller for PV system with anti-islanding grid protection: experimental realization," *IEEE Access*, vol. 7, pp. 103377–103389, 2019, doi: 10.1109/ACCESS.2019.2931547.

[23]   B. Yang *et al.*, "Novel bio-inspired memetic salp swarm algorithm and application to MPPT for PV systems considering partial shading condition," *Journal of Cleaner Production*, vol. 215, pp. 1203–1222, Apr. 2019, doi: 10.1016/j.jclepro.2019.01.150.

[24]   J. Ahmed and Z. Salam, "An enhanced adaptive P&O MPPT for fast and efficient tracking under varying environmental conditions," *IEEE Transactions on Sustainable Energy*, vol. 9, no. 3, pp. 1487–1496, Jul. 2018, doi: 10.1109/TSTE.2018.2791968.

[25]   A. Fathy, H. Rezk, and D. Yousri, "A robust global MPPT to mitigate partial shading of triple-junction solar cell-based system using manta ray foraging optimization algorithm," *Solar Energy*, vol. 207, pp. 305–316, Sep. 2020, doi: 10.1016/j.solener.2020.06.108.

[26]   L. Shang, H. Guo, and W. Zhu, "An improved MPPT control strategy based on incremental conductance algorithm," *Protection and Control of Modern Power Systems*, vol. 5, no. 1, Jun. 2020, doi: 10.1186/s41601-020-00161-z.

[27]   H. Rezk *et al.*, "A novel statistical performance evaluation of most modern optimization-based global MPPT techniques for partially shaded PV system," *Renewable and Sustainable Energy Reviews*, vol. 115, p. 109372, Nov. 2019, doi: 10.1016/j.rser.2019.109372.

[28]   M. Mansoor, A. F. Mirza, and Q. Ling, "Harris hawk optimization-based MPPT control for PV systems under partial shading conditions," *Journal of Cleaner Production*, vol. 274, p. 122857, Nov. 2020, doi: 10.1016/j.jclepro.2020.122857.

[29]   L. Guo, Z. Meng, Y. Sun, and L. Wang, "A modified cat swarm optimization based maximum power point tracking method for photovoltaic system under partially shaded condition," *Energy*, vol. 144, pp. 501–514, Feb. 2018, doi: 10.1016/j.energy.2017.12.059.

[30]   T. Sudhakar Babu, N. Rajasekar, and K. Sangeetha, "Modified particle swarm optimization technique based maximum power point tracking for uniform and under partial shading condition," *Applied Soft Computing Journal*, vol. 34, pp. 613–624, Sep. 2015, doi: 10.1016/j.asoc.2015.05.029.

[31]   M. I. Mosaad, M. Osama abed el-Raouf, M. A. Al-Ahmar, and F. A. Banakher, "Maximum power point tracking of PV system based cuckoo search algorithm; review and comparison," *Energy Procedia*, vol. 162, pp. 117–126, Apr. 2019, doi: 10.1016/j.egypro.2019.04.013.

[32]   M. L. Azad *et al.*, "An efficient MPPT approach of PV systems: Incremental conduction pathway," *Indonesian Journal of Electrical Engineering and Computer Science*, vol. 15, no. 3, pp. 1189–1196, Sep. 2019, doi: 10.11591/ijeecs.v15.i3.pp1189-1196.

[33]   Y. Zou, F. Yan, X. Wang, and J. Zhang, "An efficient fuzzy logic control algorithm for photovoltaic maximum power point tracking under partial shading condition," *Journal of the Franklin Institute*, vol. 357, no. 6, pp. 3135–3149, Apr. 2020, doi: 10.1016/j.jfranklin.2019.07.015.

[34]   S. Mohammadnejad, A. Khalafi, and S. M. Ahmadi, "Mathematical analysis of total-cross-tied photovoltaic array under partial shading condition and its comparison with other configurations," *Solar Energy*, vol. 133, pp. 501–511, Aug. 2016, doi: 10.1016/j.solener.2016.03.058.

[35]   M. Z. Shams El-Dein, M. Kazerani, and M. M. A. Salama, "An optimal total cross tied interconnection for reducing mismatch losses in photovoltaic arrays," *IEEE Transactions on Sustainable Energy*, vol. 4, no. 1, pp. 99–107, Jan. 2013, doi: 10.1109/TSTE.2012.2202325.

[36]   X. S. Yang and S. Deb, "Cuckoo search via Lévy flights," in *2009 World Congress on Nature and Biologically Inspired Computing, NABIC 2009 - Proceedings*, 2009, pp. 210–214, doi: 10.1109/NABIC.2009.5393690.

[37]   A. M. Reynolds and M. A. Frye, "Free-flight odor tracking in Drosophila is consistent with an optimal intermittent scale-free search," *PLoS ONE*, vol. 2, no. 4, p. e354, Apr. 2007, doi: 10.1371/journal.pone.0000354.

[38]   R. Poli, J. Kennedy, and T. Blackwell, "Quantification and assessment of the chemical form of residual gadolinium in the brain.pdf," *Swarm Intell*, vol. 1, no. 1, pp. 33–57, Aug. 2007, doi: 10.1007/s11721-007-0002-0.

[39]   S. Radha, S. Aasha Nandhini, and R. Hemalatha, "Efficient anomaly detection system for video surveillance application in WVSN with particle swarm optimization," in *Studies in Computational Intelligence*, vol. 676, Springer International Publishing, 2017, pp. 153–177.

BIOGRAPHIES OF AUTHORS

Sally Abdulaziz 🆔 🇬 SC Ⓟ was born in Egypt in 1988. She received a B.Sc. Degree in Electronic Engineering (Industrial electronics and Control engineering) in 2010, department of Industrial Electronics and Control Engineering, Faculty of Electronic Engineering, Menoufia University. She is interested in electrical engineering work and has worked as an Electrical engineer in industrial factories. She can be contacted at email: Sally.Abdulaziz@yahoo.com.

Galal Atlam ⓘ 🔍 SC Ⓟ was born in Egypt in 1955. He received a B.Sc. Degree in Electronic Engineering (Industrial electronics and Control engineering) in 1977, and the M.Sc. Degree in Electronic Engineering (Automatic Control Engineering) in 1988, and the Ph.D. degree in Electronic Engineering (Control Engineering and Systems) in 1997, department of Industrial Electronics and Control Engineering, Faculty of Electronic Engineering, Menoufia University, From 1977 to 1988, he was a demonstrator (Teaching Assistant), in Industrial Electronics and Control Engineering Department, Faculty of Electronic Engineering, Menoufia University. From 1988 to 1997, he was an assistant lecturer in the Industrial Electronics and Control Engineering Department, Faculty of Electronic Engineering, Menoufia University. From 1997 to 2015, he was Assistant Professor in the Industrial Electronics and Control Engineering Department, Faculty of Electronic Engineering, Menoufia University. Since 2015 he has been Professor Emeritus in the Industrial Electronics and Control Engineering Department, Faculty of Electronic Engineering, Menoufia University. He can be contacted at email: Galal.atlam@el-eng.menofia.edu.eg

Gomaa Zaki ⓘ 🔍 SC Ⓟ was born in Egypt in 1954. He received a B.Sc. Degree in Electronic Engineering (Industrial electronics and Control engineering) in 1976, and the M.Sc. Degree in Electronic Engineering (Automatic Control Engineering) in 1982, and the Ph.D. degree in Electronic Engineering (Control Engineering and Systems) in 1990, Department of Industrial Electronics and Control Engineering, Faculty of Electronic Engineering, Menoufia University, From 1976 to 1982, he was a demonstrator (Teaching Assistant), in Industrial Electronics and Control Engineering Department, Faculty of Electronic Engineering, Menoufia University. From 1982 to 1990, he was an assistant lecturer in the Industrial Electronics and Control Engineering Department, Faculty of Electronic Engineering, Menoufia University. From 1990 to 2014, he was Assistant Professor in the Industrial Electronics and Control Engineering Department, Faculty of Electronic Engineering, Menoufia University. Since 2014 he has been Professor Emeritus in the Industrial Electronics and Control Engineering Department, Faculty of Electronic Engineering, Menoufia University. He can be contacted at email: gomaazaki54@yahoo.com.

Essam Nabil ⓘ 🔍 SC Ⓟ was born in Egypt in 1984. He received a B.Sc. Degree in Electronic Engineering (Industrial Electronics and Control Engineering) in 2006, and the M.Sc. Degree in Electronic Engineering (Automatic Control Engineering) in 2011, and the Ph.D. Degree in Electronic Engineering (Control Engineering and Systems) in 2016, Department of Industrial Electronics and Control Engineering, Faculty of Electronic Engineering, Menoufia University, From 2006 to 2011, he was a demonstrator (Teaching Assistant), in the Industrial Electronics and Control Engineering Department, Faculty of Electronic Engineering, Menoufia University, and Supervisor and Chairman of the Organizing and Arbitration Committees of the permanent Scientific Exhibition of Industrial Electronics and Control Engineering department, Faculty of Electronic Engineering, Menoufia University, since 2007, and he was a supervisor and Chairman of the Organizing and Arbitration Committees of FEE Robotics Club, Faculty of Electronic Engineering, Menoufia University, since 2010, he was assistant Lecturer, in the Industrial Electronics and Control Engineering Department, Faculty of Electronic Engineering, Menoufia University, from 2011 to 2016, and Assistant Professor, in Industrial Electronics and Control Engineering department, Faculty of Electronic Engineering, Menoufia University, since 2016, he was a head of Public Relations and Notification Unit, Faculty of Electronic Engineering, Menoufia University, from 2016 to 2017, and he was a head of Scientific Computing Center, Faculty of Electronic Engineering, Menoufia University, since 2017. He can be contacted at email: essam.abdelaziz@el-eng.menofia.edu.eg.